Light scattering from transparent substrates: Theory and experiment

O. Kienzle, J. Staub, and T. Tschudi
Technische Hochschule Darmstadt, Institut für Angewandte Physik, Hochschulstraße 6, 64289 Darmstadt, Federal Republic of Germany
(Received 22 November 1993)

To produce high-quality, low-scatter optical interference coatings, substrates with extremely smooth surfaces are required for deposition. For successful production surface roughness characterization of the substrates before coating is essential. Light-scattering measurement is a nondestructive and fast surface characterization technique that determines statistical surface properties such as the power-spectral-density function (PSD) and the rms roughness δ_{rms}. Scatter measurement is an accepted tool to characterize opaque surfaces and optical interference coatings. Its application to characterize the surfaces of transparent substrates — commonly used for deposition — is difficult due to the low scatter intensities of high-quality substrates and the scattering contribution of the substrate's back surface. In this paper the total scattering distribution of a transparent substrate is calculated, considering the scattering contributions of the front and the back surface. With the theoretical result obtained, PSD's of the substrate interfaces can be calculated from angle-resolved-scattering measurement and rms roughness from the total integrated scattering measurement.

I. INTRODUCTION

Ion-based deposition techniques are commonly used to produce low-scatter optical interference coatings. Thin films deposited by these techniques show almost no inherent structure. Therefore the interfaces of the interference coating are almost a replica of the coated substrate surface. Thus the scattering properties of the interference coating are strongly dependent on the surface quality of the substrate surface. Due to the great variation of surface quality which can be found even within one set of substrates produced by one manufacturer,[1,2] characterization of each substrate before cost intensive coating is necessary. In a wide field of applications transparent glass is used as substrate material.

Four problems arise when scatter measurements are performed on uncoated transparent substrates. (1) Low scatter intensities occur due to the low reflective power of the air-substrate interfaces. (2) Multiple reflections occur inside the substrate in consequence of reflections of the back surface. These are spatially separated from the reflection of the substrate's front surface and may erroneously be interpreted as scattering. (3) There is a contribution of bulk scattering from the substrate material. (4) The scattered field is the sum of the scattered fields emerging from the front and the back surface.

Problems (2), (3), and (4) are usually avoided by either coating the substrate with a high-reflective Al coating or performing the measurement on absorbing substrate material.[1] Due to the possibility of increasing surface roughness by coating the substrate[3] and the limited range of applications where absorbing or coated substrates can be used, we decided to perform the measurement directly on those substrates being used for deposition.

Problems (1) and (2) can be solved by an advanced measurement facility as described in Ref. 2. The achieved resolution limit of the described instrument measuring total integrated scattering (TIS) using an Ulbricht sphere is 0.1 ppm (1 ppm = 10^{-6}). Scatter losses as low as 0.6 ppm have been measured on a "superpolished" fused quartz substrate, corresponding to a rms surface roughness of 1 Å. The result shows that the instrument is capable of measuring the low scatter losses of high-quality transparent substrates.

For transparent substrates we measure the sum of the scatter contributions emerging from front and back surfaces. Surface roughness characterization is thus restricted to substrates with low bulk scattering with respect to surface scattering and to substrates with equally polished sides. Fused quartz substrates with front and back surfaces polished by an identical process meet these requirements,[2] since the contribution of bulk scattering is below 0.1 ppm per mm of substrate thickness. To perform roughness analysis of the substrate interfaces from light-scattering measurements, the scattering distribution of a transparent glass substrate has to be determined. The scattering distribution includes the contributions of the front and back surfaces of the substrate. The calculation of this scattering distribution is the topic of this article.

II. SCATTERING THEORY FOR A TRANSPARENT SUBSTRATE

A. Stating the problem

Vector scattering theories have been developed by different authors, describing the scattering distribution emerging from an opaque surface[4,5] and multilayer systems.[6,7] The scattering distribution is measured in terms of angle resolved scattering (ARS), being the scattered flux in direction θ, ϕ normalized to the detector's

solid angle $d\Omega$ and the incident light flux P_0:

$$\mathcal{S} = \frac{dP_s(\theta,\phi)}{d\Omega P_0}. \quad (1)$$

When the surface roughness is assumed to be much smaller than the illuminating wavelength λ, the measured scattering distribution is proportional to the surface power-spectral-density function (PSD) in case of an opaque surface.

$$\mathcal{S} = O_F G(\vec{k}_\perp - \vec{k}_\perp^0). \quad (2)$$

The proportionality factor O_F is called the optical factor and depends on the wavelength of the incident light, the polarization states of incident and scattered light, the measurement geometry (see Fig. 3 below), and the refractive indices of the incident medium n_1 and the sample n_2. Knowledge of the optical factor enables the surface PSD $[G(\vec{k}_\perp - \vec{k}_\perp^0)]$ to be calculated from ARS measurements.

A transparent substrate consists of two boundaries separated by a distance of a few millimeters. The illuminating light beam strikes the front surface, causing a scattering distribution as defined in Eq. (2). Part of the beam will be transmitted, striking the back surface, and will cause an additional scattering distribution. The sum of both distributions is detected.[8] The detected scattering distribution measuring a transparent substrate, neglecting multiple reflections, can be defined as follows:

$$\mathcal{S} = O_F^f G^f(\vec{k}_\perp - \vec{k}_\perp^0) + O_F^b G^b(\vec{k}_\perp - \vec{k}_\perp^0). \quad (3)$$

$O_F^f G^f$ is the scattering contribution of the front surface and $O_F^b G^b$ of the back surface, respectively. The problem solved in this article is to calculate the optical factors of the two surfaces. A model for the scattering process of an opaque surface will be described first. The result obtained is the optical factor of the front surface. This optical factor can be disassembled into two parts describing the influence of the electric field on the interface caused by the incident light beam and the reactive effect of the interface on the scattered field. With this knowledge, the model will be applied to the scattering process at the back surface of the substrate.

B. Scattering theory for an opaque surface

With the assumption that the roughness is much smaller than the wavelength of the incident light ($|S(x',y')| \ll \lambda$), the scattered field can be calculated with a perturbation method limited to the first order as done by various authors.[4,9,10] A more illustrative calculation of the scattered field will be explained in this section. The calculation method can then be applied easily to the scattering process at the back surface.

The calculation can be separated into three parts. (1) As the height irregularities are small in respect to the wavelength of the incident light, the rough interface can be replaced by an ideal flat interface in the plane $z = 0$ and a distribution of surface current in this plane. (2) The scattered field at the point of observation $\vec{R}$ is calculated in the far zone approximation directly from the vector potential $\vec{A}(\vec{R})$ caused by the surface current. (3) The reactive effect of the interface on the scattered field will be taken into account.

1. *Replacement of the rough surface by a surface current density in a flat interface*

The situation is sketched in Fig. 1(a) in a one-dimensional representation. The rough interface represented by its surface topographic function $z = S(x',y')$ separates the two media with dielectric constants ϵ_1 and ϵ_2. The media are assumed to be isotropic and nonmagnetic. The interface is illuminated by a plane wave incident from medium 1, with the illuminated area being much smaller than the expansion of the interface in the x',y' direction. The scattered light will be detected in the half space containing the direction of reflection, i.e., in medium 1. In the calculation quantities related to the scattered field are indicated by index $^{(1)}$, and quantities related to the ideal flat interface by index $^{(0)}$. The calculation is performed in the cgs system.

The electric field $\vec{E}_i^{(0)}$ caused by the incident light gives rise to a polarization density $\vec{P}_i$ in the two media $i = 1, 2$,

$$\vec{P}_i = \chi_i \vec{E}_i^{(0)} = \frac{\epsilon_i - 1}{4\pi} \vec{E}_i^{(0)}. \quad (4)$$

The electric field is time dependent, $\vec{E}_i^{(0)}(t) = \vec{E}_i^{(0)} e^{-iwt}$, causing the polarization density to oscillate. Thus a polarization current density $\vec{J}_i$ is induced,

$$\vec{J}_i = \frac{\partial \vec{P}_i}{\partial t} = \frac{\epsilon_i - 1}{4\pi} \frac{\partial \vec{E}_i^{(0)}}{\partial t}. \quad (5)$$

The transition of the dielectric constant at the rough interface $z = S(x',y')$ causes a respective transition of the

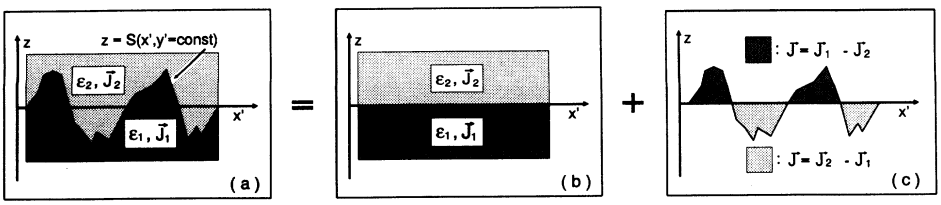

FIG. 1. Synthesis of the polarization current density distribution (CDD) at the actual interface (a) as superposition of the polarization CDD from an ideal flat interface (b) and the CDD (c). CDD (c) causes the scattered field.

polarization current density as shown in Fig. 1(a). Thus the rough interface can be described by means of a polarization current density distribution (CDD). Furthermore, it can be replaced by the sum of the polarization CDD of an ideal flat interface [Fig. 1(b)] and the CDD shown in Fig. 1(c). The flat interface (b) is defined as the mean plane of the rough interface:

$$\langle S(x',y')\rangle = \lim_{A\to\infty}\frac{1}{A}\int_A S(x',y')dx'\,dy' = 0. \tag{6}$$

Properties of this interface (reflection and transmission) are known and will be considered in their action on the incident and scattered fields only. The deviation in polarization CDD between the scattering rough interface [Fig. 1(a)] and the nonscattering flat interface [Fig. 1(b)] is the CDD $\vec{J}$ in Fig. 1(c), causing the scattered field. The CDD $\vec{J}$ is

$$\vec{J}(x',y') = \begin{cases} \vec{J}_1 - \vec{J}_2 & \text{in the region where } S(x',y') > 0, \\ \vec{J}_2 - \vec{J}_1 & \text{in the region where } S(x',y') < 0\ . \end{cases} \tag{7}$$

Phase differences of the scattered field due to different heights with respect to the flat interface can be neglected. Thus the CDD as defined in Eq. (7) is replaced by a surface CDD $\vec{J}^{(1)}$ in the flat interface $z = 0$. Its amplitude is calculated by means of conservation of the total polarization current, which is calculated on the right hand side of Eq. (8) by integrating the CDD $\vec{J}$ over the volume V, while on the left hand side it is calculated by using the surface CDD $\vec{J}^{(1)}\delta(z)$. The volume element dV is substituted by $|S(x',y')|dA$, where dA is a surface element in the $x'y'$ plane.

$$\int_V \vec{J}^{(1)}(x',y')\delta(z)dV = \int_V \vec{J}(x',y')dV,$$

$$dV = |S(x',y')|dA, \tag{8}$$

$$\int_V \vec{J}^{(1)}(x',y')\delta(z)dV$$

$$= \int_{\{A|S(x',y')>0\}} (\vec{J}_1 - \vec{J}_2)|S(x',y')|dA$$

$$+ \int_{\{A|S(x',y')<0\}} (\vec{J}_2 - \vec{J}_1)|S(x',y')|dA, \tag{9}$$

$$\int_A \vec{J}^{(1)}(x',y')dA = \int_A (\vec{J}_1 - \vec{J}_2)S(x',y')dA. \tag{10}$$

Integrating over z and substituting the CDD as defined in Eq. (7) leads to Eq. (10). This equation is valid for any integration area A; thus the integrands are equal. With Eq. (5) we obtain

$$\vec{J}^{(1)}(x',y') = S(x',y')\frac{1}{4\pi} \times\frac{\partial}{\partial t}\left[(\epsilon_1 - 1)\vec{E}_1^{(0)} - (\epsilon_2 - 1)\vec{E}_2^{(0)}\right], \tag{11}$$

$$\vec{J}^{(1)} = S(x',y')(\epsilon_1 - \epsilon_2)\frac{1}{4\pi}\frac{\partial}{\partial t}\left[\vec{E}_{t1}^{(0)} + \frac{1}{\epsilon_2}\vec{E}_{n1}^{(0)}\right]. \tag{12}$$

Here we have used the boundary conditions for the electric fields at the interface. $\vec{E}_{n1}^{(0)}$ is the normal and $\vec{E}_{t1}^{(0)}$ the tangential component of the electric field at the interface in medium 1. Equation (11) is identical to the surface CDD found by Kroeger and Kretschmann.[4] Calculating the scattered field, the roughness of the interface is involved in the amplitude of the surface current density distribution caused by the electric field at the interface. Replacing the rough interface by a distribution of surface current at the flat interface was introduced by Kroeger and Kretschmann[4] as the equivalent current model.

2. *Calculation of the scattered field*

Knowing the vector potential $\vec{A}(\vec{R})$ at the observation point $\vec{R}$ (Fig. 2) caused by the CDD, we can calculate the scattered field. The vector potential at point $\vec{R}$ is (see Ref. 11, p. 462)

$$\vec{A}(\vec{R}) = \int_G \frac{e^{ikr}}{cr}\vec{J}(\vec{r}')dV. \tag{13}$$

Using the far zone approximation ($R \gg r', kr \gg 1$) and integrating over z' we obtain for the scattered magnetic field $\vec{B}^{(1)}$

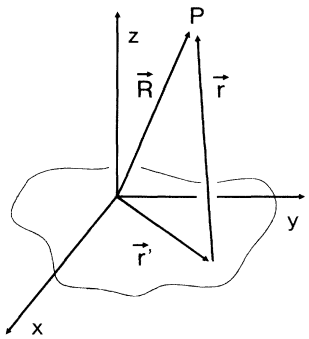

FIG. 2. Geometry for calculating the vector potential $\vec{A}$ caused by the surface CDD located in the $z = 0$ plane. $\vec{R} = (x,y,z)$, vector from origin to observation point P. $\vec{r}' = (x',y',0)$, vector from origin to point inside the CDD. $\vec{r} = \vec{R} - \vec{r}'$, vector from inside the CDD to observation point.

$$\vec{B}^{(1)}(\vec{R}) = \nabla_{\vec{R}} \times \vec{A}(\vec{R}) = \frac{ik}{cR} e^{ikR} \int_{x',y'} e^{-ik\vec{e}_R \cdot \vec{r}'} \times \left[\vec{e}_R \times \vec{J}^{(1)}(x',y') \right] dx'dy'. \quad (14)$$

where $\vec{e}_R = \vec{e}_k$ is the unit vector in the direction of the observer.

To proceed in the calculation, we have to substitute $\vec{J}^{(1)}$ and therefore we have to define the electric field $\vec{E}^{(0)}_{t1,n1}$ at the interface. We split the field into amplitude, amplitude distribution $D(x',y')$, phase factor of a plane wave with an angle of incidence θ_0 (Fig. 3), and harmonic time dependence:

$$\vec{E}^{(0)}_{t1,n1}(\vec{r}',t) = \vec{E}^{(0)}_{t1,n1} D(x',y') e^{i\vec{k}^{(0)}_{\perp} \cdot \vec{r}'} e^{-i\omega t},$$
$$\frac{\partial}{\partial t} \vec{E}^{(0)}_{t1,n1}(\vec{r}',t) = -i\omega \, \vec{E}^{(0)}_{t1,n1}(\vec{r}',t). \quad (15)$$

By introducing the amplitude distribution of the incident light beam we can exceed the limits of integration to infinity,

$$\vec{B}^{(1)}(\vec{R}) = \frac{(\epsilon_1 - \epsilon_2)}{4\pi} k^2 \frac{e^{ikR - i\omega t}}{R} \vec{e}_k \times \left[\vec{E}^{(0)}_{t1} + \frac{1}{\epsilon_2} \vec{E}^{(0)}_{n1} \right] \times \int_{-\infty}^{+\infty} \int_{-\infty}^{+\infty} e^{i(\vec{k}^{(0)}_{\perp} - \vec{k}_{\perp}) \cdot \vec{r}'} \times D(x',y') \, S(x',y') \, dx'dy'. \quad (16)$$

The integral is the Fourier transform of the product of the surface topographic function $S(x',y')$ with the amplitude distribution $D(x',y')$ and will be abbreviated as $g(\vec{k}^{(0)}_{\perp} - \vec{k}_{\perp})$.

Now we can calculate the scattered electric field $\vec{E}^{(1)}$ in medium 1:

$$\vec{E}^{(1)}(\vec{R}) = \frac{1}{n_1} \vec{B}^{(1)} \times \vec{e}_k \quad (17)$$

$$= C_1 \left\{ \left[\vec{E}^{(0)}_{t1} + \frac{1}{\epsilon_2} \vec{E}^{(0)}_{n1} \right] - \left(\left[\vec{E}^{(0)}_{t1} + \frac{1}{\epsilon_2} \vec{E}^{(0)}_{n1} \right] \cdot \vec{e}_k \right) \vec{e}_k \right\}, \quad (18)$$

$$C_1 = \frac{(\epsilon_1 - \epsilon_2)}{4\pi n_1} k^2 \frac{e^{ikR - i\omega t}}{R} g(\vec{k}^{(0)}_{\perp} - \vec{k}_{\perp}) \quad \text{with } k = \frac{\omega}{c}. \quad (19)$$

Figure 3 shows the scattering geometry. The scattered field is split into the components parallel and perpendicular to the normal $\vec{n}$ of the scattering plane. We obtain the s- and p-polarized components of the scattered field $\vec{E}^{(1)}_s$ and $\vec{E}^{(1)}_p$. The s-polarized component is parallel to $\vec{n} = \vec{e}_k \times \vec{e}_z$ and the p-polarized component is parallel to $\vec{e}_k \times \vec{n}$.

$$\vec{E}^{(1)} = \vec{E}^{(1)}_s + \vec{E}^{(1)}_p = [\vec{E}^{(1)} \cdot \vec{n}]\vec{n} + [\vec{E}^{(1)} \cdot (\vec{e}_k \times \vec{n})] (\vec{e}_k \times \vec{n}),$$
$$\vec{E}^{(1)} = C_1 \left\{ \left[\left(\vec{E}^{(0)}_{t1} + \frac{1}{\epsilon_2} \vec{E}^{(0)}_{n1} \right) \cdot \vec{n} \right] \vec{n} + \left[\left(\vec{E}^{(0)}_{t1} + \frac{1}{\epsilon_2} \vec{E}^{(0)}_{n1} \right) \cdot (\vec{e}_k \times \vec{n}) \right] (\vec{e}_k \times \vec{n}) \right\} \quad (20)$$

Now we have to determine the tangential and normal components of the electric field at the interface caused by the incident light beam. Since the amplitude of the scattered field is small with respect to the incident field we calculate the unperturbed field at the flat interface. The components and the direction of the field are dependent on the polarization state of the incident light. Therefore the scattered field is split further for calculation. We obtain four polarization cases for the scattered field $\vec{E}^{(1)}_{ij}$ with i defining the polarization state of the incident light and j of the scattered light. The field at the interface in medium 1 is the sum of the incident field $\vec{E}^{0i}$ and the reflected field $\vec{E}^{0r}$,

$$\vec{E}^{(0)}_1 = \vec{E}^{0i} + \vec{E}^{0r}. \quad (21)$$

Performing the calculation, we obtain for (i) the incident field s polarized

$$\vec{E}^{0i} = E^0 \vec{n}_0,$$
$$\vec{E}^{(0)}_{t1} = E^0 \left[1 + r^{12}_s(\theta_0) \right] \vec{n}_0, \qquad \vec{E}^{(0)}_{n1} = 0, \quad (22)$$

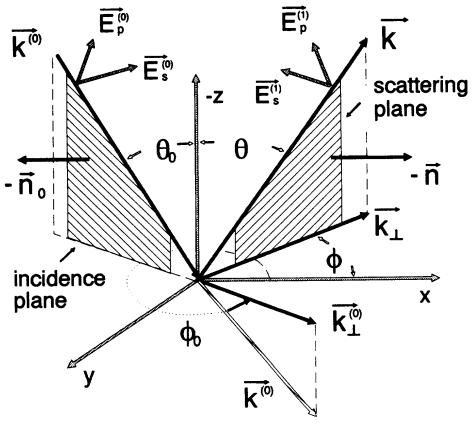

FIG. 3. Scattering geometry. The incident and scattered electric fields $\vec{E}^{(0)}$ and $\vec{E}^{(1)}$ are characterized by their propagation vectors $\vec{k}^{(0)}$ and $\vec{k}$, and their components s and p polarized with respect to the incidence plane and the scattering plane, respectively.

and (ii) the incident field p polarized

$$\begin{aligned}
\vec{E}^{0i} &= E^0[\cos\theta_0\vec{e}_{k_\perp^0} + \sin\theta_0(-\vec{e}_z)],\\
\vec{E}^{0r} &= E^0 r_p^{12}(\theta_0)\left[-\cos\theta_0\vec{e}_{k_\perp^0} + \sin\theta_0(-\vec{e}_z)\right],\\
\vec{E}_{t1}^{(0)} &= E^0\cos\theta_0[1 - r_p^{12}(\theta_0)]\vec{e}_{k_\perp^0},\\
\vec{E}_{n1}^{(0)} &= E^0\sin\theta_0[1 + r_p^{12}(\theta_0)](-\vec{e}_z). \qquad (23)
\end{aligned}$$

E^0 is the scalar amplitude of the incident field and r_s^{12} and r_p^{12} are the Fresnel amplitude coefficients of reflection for s- and p-polarized light, respectively (Appendix A). Substituting the $\vec{E}_{t1,n1}^{(0)}$ fields and performing the scalar products in Eq. (20) we obtain for the scattered field

$$\begin{aligned}
\vec{E}_{ss}^{(1)} &= C_1 E_{t1}^{(0)}\cos(\phi_0 - \phi)\vec{n},\\
\vec{E}_{sp}^{(1)} &= C_1 E_{t1}^{(0)}\cos\theta\sin(\phi_0 - \phi)\,(\vec{e}_k \times \vec{n}),\\
\vec{E}_{ps}^{(1)} &= C_1 E_{t1}^{(0)}\sin(\phi_0 - \phi)\vec{n},\\
\vec{E}_{pp}^{(1)} &= C_1\Big\{-E_{t1}^{(0)}\cos\theta\cos(\phi_0 - \phi)\\
&\quad + \frac{1}{\epsilon_2}E_{n1}^{(0)}\sin\theta\Big\}\,(\vec{e}_k \times \vec{n}). \qquad (24)
\end{aligned}$$

The result can be interpreted as the radiation characteristic of a distribution of dipole current located in free space of refractive index n_1, driven by the electric field $\vec{E} = \vec{E}_{t1}^{(0)} + 1/\epsilon_2\vec{E}_{n1}^{(0)}$. emitted field is influenced by the plane interface in its surroundings. The reaction of the interface on the emitted field will be considered in the following paragraph.

3. *Reaction of the flat interface on the scattered field*

In the described model the surface current density is located in the flat interface $z = 0$. As we have assumed a hard transition of the dielectric constant at the flat interface, we cannot define the medium in which we have to place the surface current density $\vec{J}^{(1)}$.

The ambiguity in which medium to place the scattering sources is a problem that is not restricted to the calculation method presented here. Calculations have been performed by various authors and different scattering is predicted for non-normal incident p-polarized light and p-polarized scattered light. Kroeger and Kretschmann[4] showed that a δ-function-like distribution of surface current as in Eq. (11) located in a thin intermediate vacuum layer at the interface causes field discontinuities at the flat boundary which correspond to the discontinuities calculated by Juranek[12] using first order perturbation theory. Bousquet *et al.*[7] state that the problem has an infinite number of solutions; more precisely, the surface current can be located in an intermediate layer having an arbitrarily chosen dielectric constant ϵ when the strength of the surface current is modified with respect to the dielectric constant chosen. Actually the current is located in either medium 1 or medium 2 with different strength of the polarization currents. Maradudin and Mills[9] presented a calculation method in which the scattering sources are split to be located on each side of the interface and the average value is taken to calculate the scattered field. Two different approaches have been chosen by Elson to calculate the scattering at a vacuum-material interface. In Ref. 13 the scattering currents are determined by a nonorthogonal coordinate transformation that maps the rough surface into a plane, yielding scattering currents that are not δ-function-like but extend throughout both media. In Ref. 10 the scattered field is calculated by matching the boundary conditions to first order in the surface roughness profile, which leads to discontinuities of the electric fields across the rough boundary. The results are in agreement with the result found by Kroeger and Kretschmann applied to a vacuum-material interface.

Although the calculation methods differ, the boundary conditions at the interface have to be fulfilled in any case. The question is how to perform the calculation. The approaches are (1) matching the boundary conditions at the rough interface to first order of the roughness function or (2) using the equivalent current model, replacing the rough interface by a distribution of surface current and fulfilling the boundary conditions for both the incident and scattered fields at the flat interface.

The calculation method described here is to use the equivalent current model. The boundary conditions for the incident field are fulfilled by construction. As for the scattered field, the reaction of the flat boundary on the scattered field is taken into account in order to match the boundary conditions for the electric fields. This is performed in a manner analogous to that for the incident field by using the Fresnel amplitude coefficients for reflection and transmission. Having fulfilled the boundary conditions for each polarization case and for both the incident and scattered field, the boundary conditions for the total field are fulfilled as well. Although the equivalent surface current causing the scattered field is well determined, there is the ambiguity in which medium to place the current. There are two possibilities.

(a) Placing $\vec{J}^{(1)}$ above the interface (Fig. 4). The reac-

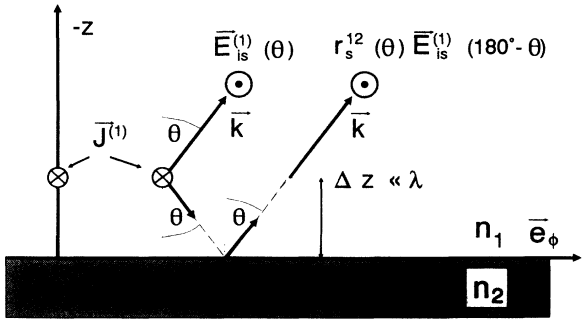

FIG. 4. Reaction of the flat interface $z = 0$ on the s-polarized scattered field $\vec{E}_{is}^{(1)}$. The surface CDD $\vec{J}^{(1)}$ is assumed to be located in medium 1, in distance $\Delta z \ll \lambda$ above the interface. The scattered field propagating in the direction $\vec{k}$ is the sum of the field emitted from $\vec{J}^{(1)}$ directly in direction θ, ϕ and the field emitted in direction $(180° - \theta)$, ϕ and reflected off the interface.

tion of the flat boundary (no multiple scattering) on the scattered field can be calculated as follows. The scattered field propagating in direction $\vec{k}$ is the sum of the field emitted from the surface CDD in direction $\vec{k}$ directly and the field emitted towards the interface and after reflection off the interface propagating also in direction $\vec{k}$.

(b) Placing $\vec{J}^{(1)}$ below the interface. The scattered field is calculated in medium 2, and the transmission of the field into medium 1 is considered.

Both possibilities are equal in terms of the described model. Referring to Fig. 1, the exact splitting of the current would be the following. The current would be located above the interface in medium 1 for the areas where $S(x',y') > 0$ and below the interface in medium 2 where $S(x',y') < 0$. Since the calculation of the scattered fields using a surface current split in this way is difficult, the surface current is split into equal parts located below and above the interface in the illuminated area. This assumption is valid in a statistical sense, because $\langle S(x',y')\rangle = 0$ and therefore half of the polarization current strength is located above and the other half below the interface. The scattered field is calculated for both locations separately and then coherently added to obtain the total scattered field.

Later on we will see that the assumption to split the surface CDD into equal parts located below and above the interface shows good agreement between theory and experiment.

We now perform the calculation.

(a) Locating the surface CDD above the interface and considering the reflection of scattered light at the interface, the scattered field with polarization state i,j defined in Eq. (24) transforms according to

$$\vec{E}_{ij}^{(1)} \rightarrow \vec{E}_{ij}^{(1)}(\theta) + r_j^{12}(\theta)\vec{E}_{ij}^{(1)}(180^\circ - \theta). \tag{25}$$

The amount of reflected scattered light is $r_j^{12}(\theta)\vec{E}_{ij}(180^\circ - \theta)$.

(b) Locating the surface CDD below the interface in medium 2, we have to calculate the scattered fields in medium 2 first. Since the wave number has changed, the propagation vector in medium 2 is $\vec{e}_{k'}$ (for the respective surface Fourier component, see Appendix B) corresponding to the scattering angles θ' and ϕ. The factor n_1/n_2 expresses the changed admittance and $(\vec{E}_{ij}^{(1)})_2$ denotes that the scattered field is calculated in medium 2.

$$\begin{aligned}
(\vec{E}_{ss}^{(1)})_2 &= \frac{n_1}{n_2} C_1 E_{t1}^{(0)} \cos(\phi_0 - \phi)\vec{n}, \\
(\vec{E}_{sp}^{(1)})_2 &= \frac{n_1}{n_2} C_1 E_{t1}^{(0)} \cos\theta' \sin(\phi_0 - \phi)\,(\vec{e}_{k'} \times \vec{n}), \\
(\vec{E}_{ps}^{(1)})_2 &= \frac{n_1}{n_2} C_1 E_{t1}^{(0)} \sin(\phi_0 - \phi)\vec{n}, \\
(\vec{E}_{pp}^{(1)})_2 &= \frac{n_1}{n_2} C_1 \Big\{ -E_{t1}^{(0)} \cos\theta' \cos(\phi_0 - \phi) \\
&\quad + \frac{1}{\epsilon_2} E_{n1}^{(0)} \sin\theta' \Big\} (\vec{e}_{k'} \times \vec{n}).
\end{aligned} \tag{26}$$

To be detected in medium 1, the scattered field has to pass the interface. The scattering angle θ' in medium 2 has to be considered in the amplitude coefficient of transmission $t_j^{21}(\theta')$. The amplitude of the scattered field with polarization state ij transforms according to

$$\left|\left(\vec{E}_{ij}^{(1)}\right)'\right| = \sqrt{\frac{\cos\theta}{\cos\theta'}} t_j^{21}(\theta') \left|\left(\vec{E}_{ij}^{(1)}\right)_2\right|. \tag{27}$$

The direction of propagation changes in $\vec{e}_k$ related to the scattering angles θ and ϕ outside the substrate.

Having calculated the scattered field for case (a) and (b), we have to express the result in terms of angle resolved scattering as defined in Eq. (1). The scattered light flux through the surface element dA perpendicular to the direction of propagation located a distance R from the illuminated surface is

$$dP_s = \frac{c}{8\pi} n_1 |\vec{E}^{(1)}|^2 dA \Rightarrow \frac{dP_s}{d\Omega} = \frac{c}{8\pi} n_1 |\vec{E}^{(1)}|^2 R^2,$$

since $dA = R^2 d\Omega$. With the incident light flux $P_0 = \frac{c}{8\pi} n_1 \cos\theta_0 |E^0|^2 \int_{-\infty}^{+\infty}\int_{-\infty}^{+\infty} |D(x',y')|^2 dx'dy'$, we obtain

$$\mathcal{S} = \frac{dP_s}{d\Omega P_0} = \frac{|\vec{E}^{(1)}|^2 R^2}{|E^0|^2 \cos\theta_0 \int_{-\infty}^{+\infty}\int_{-\infty}^{+\infty} |D(x',y')|^2 dx'dy'}.$$

Here we have to substitute the scattered field $|\vec{E}^{(1)}|$ by $\vec{E}_{ij}^{(1)}$ from Eq. (25) for placing the surface current above the interface or $(\vec{E}_{ij}^{(1)})'$ from Eq. (27) for placing it below the interface. Placing the current above the interface we obtain for the ARS of the respective polarization state

$$\frac{dP_s}{d\Omega P_0} = \frac{|(\epsilon_1 - \epsilon_2)|^2 k^4}{(4\pi)^2 n_1^2 \cos\theta_0} \frac{|g(\vec{k}_\perp - \vec{k}_\perp^{(0)})|^2}{\int_{-\infty}^{+\infty}\int_{-\infty}^{+\infty} |D(x',y')|^2 dx'dy'}$$

$$\times \begin{cases} |[1 + r_s^{12}(\theta_0)][1 + r_s^{12}(\theta)]\cos(\phi_0 - \phi)|^2, & ss, \\ |[1 + r_s^{12}(\theta_0)][1 - r_p^{12}(\theta)]\cos\theta \sin(\phi_0 - \phi)|^2, & sp, \\ |[1 - r_p^{12}(\theta_0)][1 + r_s^{12}(\theta)]\cos\theta_0 \sin(\phi_0 - \phi)|^2, & ps \\ |[1 - r_p^{12}(\theta_0)][1 - r_p^{12}(\theta)]\cos\theta_0 \cos\theta \cos(\phi_0 - \phi) \\ -\frac{1}{\epsilon_2}[1 + r_p^{12}(\theta_0)][1 + r_p^{12}(\theta)]\sin\theta_0 \sin\theta|^2, & pp\,. \end{cases} \tag{28}$$

The ARS is proportional to $|g(\vec{k}_\perp - \vec{k}_\perp^{(0)})|^2$ which is the square of the convolution of the Fourier transforms of the surface topographic function $S(x', y')$ and the amplitude distribution $D(x', y')$. Assuming a spatially constant amplitude distribution $D(x', y')$ at the interface, we get the following expression:

$$\frac{|g(\vec{k}_\perp - \vec{k}_\perp^0)|^2}{\int\int |D(x', y')|^2 dx' dy'} = \frac{1}{A}|s(\vec{k}_\perp - \vec{k}_\perp^0)|^2 \equiv G(\vec{k}_\perp - \vec{k}_\perp^0), \tag{29}$$

where A is the illuminated area. $G(\vec{k}_\perp - \vec{k}_\perp^0)$ is the power-spectral-density function of the rough surface. Thus the ARS can be written in the common form as the optical factor multiplied by the PSD of the rough surface:

$$\mathcal{S} = O_F G(\vec{k}_\perp - \vec{k}_\perp^{(0)}).$$

Looking at the optical factors, we can identify the Rayleigh scattering wavelength dependence ($O_F \sim k^4$), and the angular dipole radiation characteristics. Furthermore the factors $[1 \pm r_{s,p}^{12}(\theta_0)]$ show the dependence on the electric field at the interface caused by the incident light, and the factors $[1 \pm r_{s,p}^{12}(\theta)]$ describe the reflection of the scattered field at the interface.

When substituting the Fresnel amplitude coefficients of reflection it can be shown that the result is identical to the results quoted by other authors.[14,10]

For the polarization cases ss, sp, and ps the result is identical to the result found when the Bousquet *et al.* theory for multiple boundary systems[7] is applied to an opaque surface. A deviation of the scattered field found in the pp-polarized component can be explained by the usage of a modified surface current in the Bousquet *et al.* theory. Substituting the surface current as defined in Eq. (12), the results are identical.[15]

C. Theory for scattering from the back surface of the substrate

Knowing the mechanisms of the scattering process we can calculate the scattering distribution of the substrate's back surface (Fig. 5). The illuminating light incident from medium 1, angle of incidence θ_0, transmits through the front surface (interface f) and causes an electric field at the back surface (interface b). Interface b is assumed to be rough. A given Fourier component of the surface causes the scattered wave with amplitude $[\vec{E}^{(1)b}]_2$ inside the substrate. The direction of propagation is $\vec{e}_{k'}$, related to the scattering angles θ', ϕ. The scattered wave transmits through interface f in medium 1 where it is detected. The amplitude changes in $[\vec{E}^{(1)b}]_1$ and the propagation vector changes due to refraction in $\vec{e}_k$ related to the scattering angles θ, ϕ outside the substrate.

Starting the calculation, we have to calculate the electric field at interface b caused by the incident light. The calculation is performed by analogy with Eqs. (22) and (23), taking into account the transmission coefficients $t^{12}(\theta_0)$ for the transmission of the field through interface f and the incidence angle θ_0' upon interface b. For the amplitudes of the electric field at interface b in medium 2 we obtain

$$E_{t2}^{(0)b} = E^0 \begin{cases} t_s^{12}(\theta_0)\left[1 + r_s^{21}(\theta_0'),\right], & \text{incident light } s \text{ polarized,} \\ t_p^{12}(\theta_0)\cos\theta_0'\left[1 - r_p^{21}(\theta_0')\right], & \text{incident light } p \text{ polarized,} \end{cases} \tag{30}$$

$$E_{n2}^{(0)b} = E^0 \begin{cases} 0, & \text{incident light } s \text{ polarized,} \\ t_p^{12}(\theta_0)\sin\theta_0'\left[1 + r_p^{21}(\theta_0')\right], & \text{incident light } p \text{ polarized,} \end{cases} \tag{31}$$

where E^0 is the amplitude of the field incident from medium 1.

Considering the reaction of interface b on the scattered field, we have again two possibilities.

(a) Placing the surface current above the interface into medium 2 the scattered field inside the substrate in the absence of the flat interface is

$$\begin{aligned}
\left[\vec{E}_{ss}^{(1)b}\right]_2 &= C^b E_{t2}^{(0)b}\cos(\phi_0 - \phi)\vec{n}, \\
\left[\vec{E}_{sp}^{(1)b}\right]_2 &= C^b E_{t2}^{(0)b}\cos\theta'\sin(\phi_0 - \phi)(\vec{e}_{k'} \times \vec{n}), \\
\left[\vec{E}_{ps}^{(1)b}\right]_2 &= C^b E_{t2}^{(0)b}\sin(\phi_0 - \phi)\vec{n}, \\
\left[\vec{E}_{pp}^{(1)b}\right]_2 &= C^b\Big\{-E_{t2}^{(0)b}\cos\theta'\cos(\phi_0 - \phi) \\
&\quad + \frac{1}{\epsilon_1}E_{n2}^{(0)b}\sin\theta'\Big\}(\vec{e}_{k'} \times \vec{n}),
\end{aligned}$$

$$C^b = \frac{(\epsilon_2 - \epsilon_1)}{4\pi n_2}k^2\frac{e^{ikR - iwt}}{R}\, g^b(\vec{k}_\perp^{(0)} - \vec{k}_\perp),$$

$$g^b(\vec{k}_\perp^{(0)} - \vec{k}_\perp) = \int_{-\infty}^{+\infty}\int_{-\infty}^{+\infty} e^{i(\vec{k}_\perp^{(0)} - \vec{k}_\perp)\cdot\vec{r}'} \times D^b(x', y')\, S^b(x', y')dx'dy'. \tag{32}$$

$g^b(\vec{k}_\perp^{(0)} - \vec{k}_\perp)$ (the argument is left unchanged, see Appendix B) is the Fourier transform of the product of the surface topographic function of the back surface (interface b) with the corresponding amplitude distribution. The scattering direction inside the substrate is $\vec{e}_{k'}$ related to the scattering angles θ' and ϕ. The $1/n_2$ factor

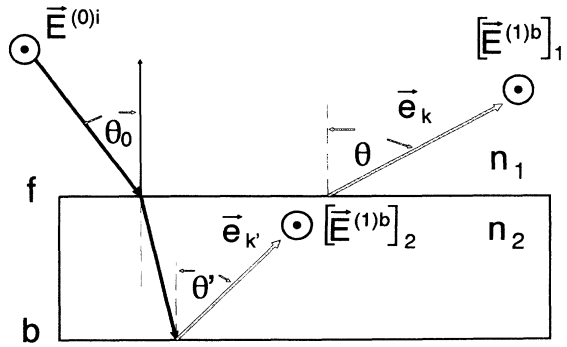

FIG. 5. Scattering process at the back surface of the substrate. The light incident from medium 1 transmits into the substrate, causing an electric field at interface b. The rough interface b causes the scattered field $[\vec{E}^{(1)b}]_2$ inside the substrate. The scattered field passes through interface f having the amplitude $[\vec{E}^{(1)b}]_1$ in medium 1 where it is detected.

in C^b expresses the changed admittance inside the substrate. Considering the reflection of the scattered light at interface b, the scattered field transforms according to

$$\left[\vec{E}_{ij}^{(1)b}(\theta')\right]_2 \rightarrow \left[\vec{E}_{ij}^{(1)b}(\theta')\right]_2 + r_j^{21}(\theta')\left[\vec{E}_{ij}^{(1)b}(180^\circ - \theta')\right]_2 . \quad (33)$$

(b) Placing the surface current below the interface, we have to calculate the scattered field in medium 1 (propagation direction $\vec{e}_k$) first:

$$\left[\vec{E}_{ss}^{(1)b}\right]_1 = \frac{n_2}{n_1} C^b E_{t2}^{(0)b} \cos(\phi_0 - \phi)\vec{n},$$

$$\left[\vec{E}_{sp}^{(1)b}\right]_1 = \frac{n_2}{n_1} C^b E_{t2}^{(0)b} \cos\theta \sin(\phi_0 - \phi)\,(\vec{e}_k \times \vec{n}),$$

$$\left[\vec{E}_{ps}^{(1)b}\right]_1 = \frac{n_2}{n_1} C^b E_{t2}^{(0)b} \sin(\phi_0 - \phi)\vec{n},$$

$$\left[\vec{E}_{pp}^{(1)b}\right]_1 = \frac{n_2}{n_1} C^b \left\{ -E_{t2}^{(0)b} \cos\theta \cos(\phi_0 - \phi) + E_{n2}^{(0)b} \frac{1}{\epsilon_1} \sin\theta \right\} (\vec{e}_k \times \vec{n}),$$

and then we have to take into account the transmission of the scattered field through interface b into the substrate. The propagation vector changes into $\vec{e}_{k'}$ and the amplitude of the scattered field with polarization state ij transforms according to

$$\left|\left[\vec{E}_{ij}^{(1)b}\right]_2'\right| = \sqrt{\frac{\cos\theta'}{\cos\theta}}\, t_j^{12}(\theta) \left|\left[\vec{E}_{ij}^{(1)b}\right]_1\right|. \quad (34)$$

To be detected in medium 1, the scattered fields which were calculated in medium 2 have to pass through the interface f. We obtain for the amplitude of the field scattered from the back surface detected in medium 1

$$\left|\left[\vec{E}_{ij}^{(1)b}\right]_1\right| = \sqrt{\frac{\cos\theta}{\cos\theta'}}\, t_j^{21}(\theta') \left|\left[\vec{E}_{ij}^{(1)b}\right]_2\right| . \quad (35)$$

Here we have to insert the scattered field inside the substrate as defined in Eqs. (33) or (34) for placing the surface current above or below the interface. Dividing the calculated scattered flux in medium 1 by the incident flux from medium 1, we obtain for the ARS of the back surface

$$\left(\frac{dP_s}{d\Omega P_0}\right)^b = \frac{\left|\left[\vec{E}^{(1)b}\right]_1\right|^2 R^2}{|E^0|^2 \cos\theta_0' \int_{-\infty}^{+\infty}\int_{-\infty}^{+\infty} |D^b(x',y')|^2 dx'dy'}. \quad (36)$$

The result for placing the surface current above the interface b is given in Eq. (37). Using Eq. (29) it can be identified as the optical factor of the back surface O_F^b multiplied by its power spectral density function $G^b(\vec{k}_\perp - \vec{k}_\perp^{(0)})\mathcal{P}^b$.

$$\left(\frac{dP_s}{d\Omega P_0}\right)^b = \frac{|\,(\epsilon_1 - \epsilon_2)\,|^2\, k^4}{(4\pi)^2 n_2^2 \cos\theta_0'} \frac{|\,g^b(\vec{k}_\perp - \vec{k}_\perp^{(0)})\,|^2}{\int_{-\infty}^{+\infty}\int_{-\infty}^{+\infty} |\,D^b(x',y')\,|^2\, dx'dy'}$$

$$\times \begin{cases} |\,t_s^{12}(\theta_0)\,[1 + r_s^{21}(\theta_0')]\,[1 + r_s^{21}(\theta')]\sqrt{\frac{\cos\theta}{\cos\theta'}}\, t_s^{21}(\theta')\cos(\phi_0 - \phi)\,|^2, & ss, \\ |\,t_s^{12}(\theta_0)\,[1 + r_s^{21}(\theta_0')]\,[1 - r_p^{21}(\theta')]\sqrt{\frac{\cos\theta}{\cos\theta'}}\, t_p^{21}(\theta')\cos\theta'\sin(\phi_0 - \phi)\,|^2, & sp, \\ |\,t_p^{12}(\theta_0)\,[1 - r_p^{21}(\theta_0')]\cos\theta_0'[1 + r_s^{21}(\theta')]\sqrt{\frac{\cos\theta}{\cos\theta'}}\, t_s^{21}(\theta')\sin(\phi_0 - \phi)\,|^2, & ps, \\ |\,t_p^{12}(\theta_0)\{-[1 - r_p^{21}(\theta_0')]\cos\theta_0'[1 - r_p^{21}(\theta')]\cos\theta'\cos(\phi_0 - \phi) \\ \quad + \frac{1}{\epsilon_1}\sin\theta_0'[1 + r_p^{21}(\theta_0')][1 + r_p^{21}(\theta')]\sin\theta'\}\sqrt{\frac{\cos\theta}{\cos\theta'}}\, t_p^{21}(\theta')\,|^2, & pp \end{cases} \quad (37)$$

with $\cos\theta' = (1/n_2)\sqrt{n_2^2 - n_1^2\sin\theta}$ $\sin\theta' = (n_1/n_2)\sin\theta$.

D. Comparison of optical factors of front and back surfaces

In Fig. 6 optical factors for the front surface and the back surface of a fused quartz substrate ($n_2 = 1.46, n_1 = 1$) are shown in dependence on the scattering angle θ. In the calculation the wavelength is $\lambda = 633$ nm, the angle of incidence is $\theta_0 = 0$, and the angle between the incidence and the scattering plane is $\phi - \phi_0 = 0$.

The location of the surface current influences the angular dependence of the optical factors for scattering angles above $\approx 20^\circ$, caused by the angular dependence of the coefficients for reflection and transmission. The most important result is that the optical factor of the back surface is greater than the optical factor of the front surface, which is independent of the location of the surface current. Since the difference in dielectric constants is identical for both interfaces, this result is not obvious. The explanation is as follows. Using the identity $[1 + r_s^{21}(\theta_i')] = [1 - r_s^{12}(\theta_i)]$ we obtain the following quotient of the optical factors for ss polarization and normal incidence illumination for placing the surface current densities above each interface:

$$\frac{O_F^b}{O_F^f} = \frac{|t_s^{12}(0)\sqrt{\frac{\cos(\theta)}{\cos(\theta')}}t_s^{21}(\theta')|^2 \left|[1-r_s^{12}(0)][1-r_s^{12}(\theta)]\right|^2 \frac{1}{n_2^2}}{\left|[1+r_s^{12}(0)][1+r_s^{12}(\theta)]\right|^2 \frac{1}{n_1^2}}, \tag{38}$$

since

$$[1-r_s^{12}(0)] = \frac{n_2}{n_1}[1+r_s^{12}(0)]. \tag{39}$$

We obtain

$$\frac{O_F^b}{O_F^f} = \frac{T^{12}(0)T^{21}(\theta') \left|[1+r_s^{12}(0)][1-r_s^{12}(\theta)]\right|^2 \frac{1}{n_1^2}}{\left|[1+r_s^{12}(0)][1+r_s^{12}(\theta)]\right|^2 \frac{1}{n_1^2}}. \tag{40}$$

Equation (40) shows that the scattering process at the back surface can be written corresponding to the scattering process at the front surface considering the transmitted power coefficients for the incident light $T^{12}(0)$ and the scattered light $T^{21}(\theta')$, and the phase shifts of the reflected scattered light. For non-conducting media the phase shift of the reflected scattered light is $\Delta\phi = \pi$ since $n_2 > n_1$ at the front surface and $\Delta\phi = 0$ at the back surface. Summation of the directly emitted scattered light and the reflected scattered light is destructive for the front surface ($[1+r_s^{12}(\theta)]$, with $r_s^{12} < 0$) and constructive for the back surface ($[1-r_s^{12}(\theta)]$). This explains the difference in the optical factors.

Using Eq. (39) the quotient of the optical factors for small scattering angles becomes

$$\frac{O_F^b}{O_F^f}(\theta_0 = 0, \theta = 0) = T^{12}(0)T^{21}(0)\frac{n_2^2}{n_1^2}, \tag{41}$$

which is independent of the location of the surface current density. Assuming a fused quartz substrate and equal surface roughness of the interfaces, the contribution of scattered light intensity from the back surface is a factor 1.98 greater than the contribution of the front surface.

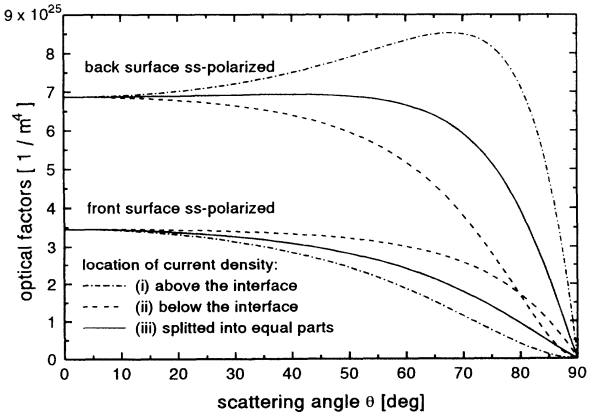

FIG. 6. Comparison of calculated optical factors (ss polarized, $\lambda = 633$ nm, $\theta_0 = 0, \phi - \phi_0 = 0$) of the front and the back surface of a fused quartz substrate. They were calculated for three locations of the surface current density distribution with respect to the flat interface $z = 0$.

E. Comparison between theory and experiment

The result of the theoretical model describing the stray-light emission of the back surface of a transparent substrate has been confirmed by measurement. Measurement is carried out by means of an ARS instrument built at our institute[15] based on the experimental setup as described in Ref. 2. The geometry defining the scattering angles is related to common conventions as described, for instance, in Ref. 7.

Figure 7 shows the ARS measurements of two fused quartz substrates with different polishing specifications, polished by the same manufacturer. Substrate 1 is specified as one side "superpolished," and the other side is unspecified. Substrate 2 is specified as "superpolished" on both sides. The scattering contribution of the superpolished interface can be neglected, as can be seen from comparison of the measurements. Thus substrate 1 can be described as having just one rough surface. As the measurement of substrate 1 was carried out with opposite orientations of the surfaces with respect to the incident beam, we can see the difference in the optical factors. We obtain two cases for ARS from a substrate with one rough interface having the power spectral density function $G^r(\vec{k}_\perp - \vec{k}_\perp^0)$.

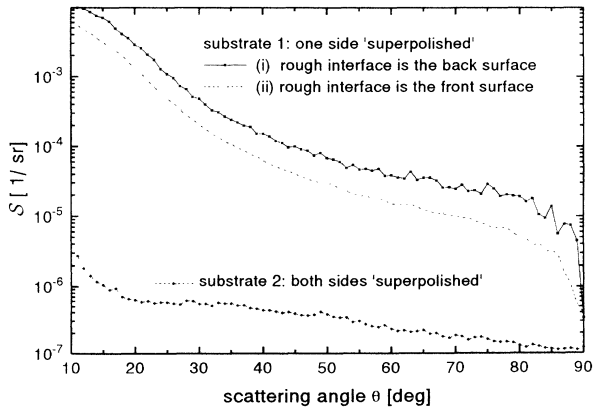

FIG. 7. Measured ARS of two substrates with different polishing specifications. The major scattering contribution of substrate 1 is caused by the unspecified (rough) surface only. Measurement of substrate 1 was carried out with opposite orientations: (i) the rough interface is the back surface and (ii) the rough interface is the front surface. Measurement parameters are polarization ss, $\lambda = 633$ nm, $\theta_0 = 8°, \phi - \phi_0 = 0$.

(i) The rough surface is the back surface

$$\mathcal{S}^b = O_F^b G^r(\vec{k}_\perp - \vec{k}_\perp^0).$$

(ii) The rough surface is the front surface

$$\mathcal{S}^f = O_F^f G^r(\vec{k}_\perp - \vec{k}_\perp^0).$$

The measurement confirms that the optical factor of the back surface is a factor of 2 greater than the optical factor of the front surface, since the PSD's in both measurements are identical. Comparing the quotient of the ARS curves with the quotient of the optical factors calculated by means of the described model, we can perform a more detailed analysis clarifying the location of the surface current. The quotient of the ARS curves for the two orientations is

$$\frac{\mathcal{S}^b}{\mathcal{S}^f} = \frac{O_F^b}{O_F^f}. \tag{42}$$

This enables us to determine the quotient of the optical factors by means of ARS measurement of a substrate with one rough surface. The measured quotient is plotted in Fig. 8, curve (iv). The calculated quotients [curves (i)–(iii) of Fig. 8] correspond to different locations of the surface current. (i) The surface current is located above each interface and (ii) the surface current is located below each interface. Curve (iii) shows the quotient for splitting the surface current on each interface into equal parts above and below the corresponding interface and calculating the scattered field as the sum of the scattered fields emitted by the two parts. Comparison with the measured quotient [curve (iv)] shows a very good agreement between theory and experiment for splitting the surface current distribution into equal parts. This result is reasonable in terms of the described model. Since we assumed a hard transition of the dielectric constant at the plane $z = 0$, it is not possible to decide in which medium we have to place the current density. Referring to Fig. 1(a), the exact location of the surface current

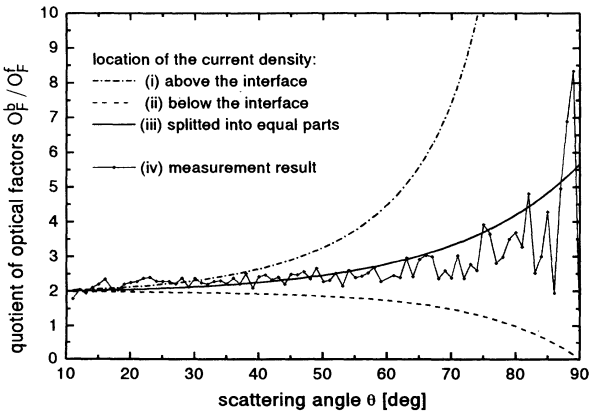

FIG. 8. Comparison of the quotient of the optical factors calculated by means of the described model. Results for three locations of the current density (i)–(iii) with respect to the flat interface are compared with the measured quotient (iv).

is above the interface in medium 1 when $S(x', y') > 0$, and below the interface in medium 2 when $S(x', y') < 0$. Calculation of the scattered field in this way runs into difficulties. Splitting the surface current into equal parts above and below the interface corresponds to the actual location rather than the location at one side of the interface only, which is confirmed by the measurement result.

For the total scattering distribution of a transparent substrate we obtain:

$$\mathcal{S} = \left(\frac{dP_s}{d\Omega P_0}\right)^f + \left(\frac{dP_s}{d\Omega P_0}\right)^b,$$

with the contributions of the front and the back surface defined by Eqs. (46) and (47), respectively. The scattering contributions caused by the amount of incident and scattered light that is (multiply) reflected inside the substrate are not considered in this theory, since they are at least one order of magnitude smaller than the calculated contributions.

For a spatially constant amplitude distribution we can use Eq. (29) and write the ARS in dependence on the optical factors and the surface's power-spectral-density functions as

$$\mathcal{S} = O_F^f G^f(\vec{k}_\perp^0 - \vec{k}_\perp) + O_F^b G^b(\vec{k}_\perp^0 - \vec{k}_\perp). \tag{43}$$

Two measurements can be performed with opposite orientations of the substrate in respect to the incident beam when the PSD's differ. The PSD of the front and back surfaces can be determined separately, due to the different optical factors. Assuming $\mathcal{S}_\mathrm{I}$ to be the measurement with surface I [the PSD is $G_\mathrm{I}(\vec{k}_\perp^0 - \vec{k}_\perp)$] as front surface and $\mathcal{S}_\mathrm{II}$ with surface II [the PSD is $G_\mathrm{II}(\vec{k}_\perp^0 - \vec{k}_\perp)$] as front surface, the ARS of the two measurements is

$$\mathcal{S}_\mathrm{I} = O_F^f G_I(\vec{k}_\perp^0 - \vec{k}_\perp) + O_F^b G_\mathrm{II}(\vec{k}_\perp^0 - \vec{k}_\perp),$$
$$\mathcal{S}_\mathrm{II} = O_F^f G_\mathrm{II}(\vec{k}_\perp^0 - \vec{k}_\perp) + O_F^b G_\mathrm{I}(\vec{k}_\perp^0 - \vec{k}_\perp).$$

For the PSD's this can be solved in matrix form:

$$\begin{pmatrix} G_\mathrm{I} \\ G_\mathrm{II} \end{pmatrix} = [[O_F^f]^2 - [O_F^b]^2]^{-1} \begin{pmatrix} O_F^f & -O_F^b \\ -O_F^b & O_F^f \end{pmatrix} \begin{pmatrix} \mathcal{S}_\mathrm{I} \\ \mathcal{S}_\mathrm{II} \end{pmatrix}. \tag{44}$$

This measuring technique is restricted to substrates with slightly varying PSD's with respect to different locations on the surface, since we cannot generally ensure that we measure the same locations on the surfaces in both measurements. Substrates of high polishing quality reach this demand. For each orientation several locations can be measured, and the statistical averages can be used for calculating the PSD's.

The result can be simplified for substrates with equally polished sides corresponding to equal PSD's $\widehat{G}(\vec{k}_\perp^0 - \vec{k}_\perp)$ of the surfaces:

$$\widehat{\mathcal{S}} = [O_F^f + O_F^b]\widehat{G}(\vec{k}_\perp^0 - \vec{k}_\perp). \tag{45}$$

F. Results for splitting the surface currents into equal parts

(i) Results for the front surface

$$\left(\frac{dP_s}{d\Omega P_0}\right)^f = \frac{|(\epsilon_1-\epsilon_2)|^2\,k^4}{(4\pi)^2 n_1^2\cos\theta_0}\frac{|g^f(\vec{k}_\perp-\vec{k}_\perp^{(0)})|^2}{\int_{-\infty}^{+\infty}\int_{-\infty}^{+\infty}|D^f(x',y')|^2dx'dy'}$$

$$\times\begin{cases}\left|\,|\frac{1}{2}[1+r_s^{12}(\theta_0)]\,\{\,[1+r_s^{12}(\theta)]+\frac{n_1}{n_2}\sqrt{\frac{\cos\theta}{\cos\theta'}}[1-r_s^{12}(\theta)]\,\}\cos(\phi_0-\phi)\,\right|^2, & ss,\\ \left|\,\frac{1}{2}[1+r_s^{12}(\theta_0)]\,\{\,[1-r_p^{12}(\theta)]\cos\theta+\sqrt{\frac{\cos\theta}{\cos\theta'}}[1-r_p^{12}(\theta)]\cos\theta'\,\}\sin(\phi_0-\phi)\,\right|^2, & sp,\\ \left|\,\frac{1}{2}[1-r_p^{12}(\theta_0)]\cos\theta_0\,\{\,[1+r_s^{12}(\theta)]+\frac{n_1}{n_2}\sqrt{\frac{\cos\theta}{\cos\theta'}}[1-r_s^{12}(\theta)]\,\}\sin(\phi_0-\phi)\,\right|^2, & ps,\\ \left|\,\frac{1}{2}\Big[\,[1-r_p^{12}(\theta_0)]\cos\theta_0\cos(\phi_0-\phi)\,\{\,[1-r_p^{12}(\theta)]\cos\theta+\sqrt{\frac{\cos\theta}{\cos\theta'}}[1-r_p^{12}(\theta)]\cos\theta'\,\}\right.\right.\\ \left.\left.-\frac{1}{\epsilon_2}[1+r_p^{12}(\theta_0)]\sin\theta_0\,\{\,[1+r_p^{12}(\theta)]\sin\theta+\sqrt{\frac{\cos\theta}{\cos\theta'}}[1-r_p^{12}(\theta)]\sin\theta'\,]\,\}\Big]\right|^2, & pp.\end{cases} \tag{46}$$

(ii) Result for the back surface

$$\left(\frac{dP_s}{d\Omega P_0}\right)^b = \frac{|\,(\epsilon_1-\epsilon_2)\,|^2\;k^4}{(4\pi)^2 n_2^2\cos\theta_0'}\frac{\cos\theta}{\cos\theta'}\frac{|\,g^b(\vec{k}_\perp-\vec{k}_\perp^{(0)})\,|^2}{\int_{-\infty}^{+\infty}\int_{-\infty}^{+\infty}|\,D^b(x',y')\,|^2\,dx'dy'}$$

$$\times\begin{cases}\left|\,\frac{1}{2}t_s^{12}(\theta_0)[1-r_s^{12}(\theta_0)][1-r_s^{12}(\theta)]\times\left\{\,[1-r_s^{12}(\theta)]+\frac{n_2}{n_1}\sqrt{\frac{\cos\theta'}{\cos\theta}}t_s^{12}(\theta)\,\right\}\cos(\phi_0-\phi)\,\right|^2, & ss,\\ \left|\,\frac{1}{2}t_s^{12}(\theta_0)[1-r_s^{12}(\theta_0)]\frac{n_2}{n_1}[1-r_p^{12}(\theta)]\right.\\ \left.\times\left\{\,[1+r_p^{12}(\theta)]\cos\theta'+\frac{n_2}{n_1}\sqrt{\frac{\cos\theta'}{\cos\theta}}t_p^{12}(\theta)\cos\theta\,\right\}\sin(\phi_0-\phi)\,\right|^2, & sp,\\ \left|\,\frac{1}{2}t_p^{12}(\theta_0)[1+r_p^{12}(\theta_0)]\cos\theta_0'[1-r_s^{12}(\theta)]\times\left\{\,[1-r_s^{12}(\theta)]+\frac{n_2}{n_1}\sqrt{\frac{\cos\theta'}{\cos\theta}}t_s^{12}(\theta)\,\right\}\sin(\phi_0-\phi)\,\right|^2, & ps,\\ \left|\,\frac{1}{2}t_p^{12}(\theta_0)\frac{n_2}{n_1}[1-r_p^{12}(\theta)\right.\\ \left.\times\Big[\,\cos\theta_0'\cos(\phi_0-\phi)[1+r_p^{12}(\theta_0)]\,\{\,[1+r_p^{12}(\theta)]\cos\theta'+\frac{n_2}{n_1}\sqrt{\frac{\cos\theta'}{\cos\theta}}t_p^{12}(\theta)\cos\theta\,\}\right.\right.\\ \left.\left.-\frac{1}{\epsilon_1}\sin\theta_0'[1-r_p^{12}(\theta_0)]\,\{\,[1-r_p^{12}(\theta)]\sin\theta'+\frac{n_2}{n_1}\sqrt{\frac{\cos\theta'}{\cos\theta}}t_p^{12}(\theta)\sin\theta\,\}\Big]\right|^2, & pp.\end{cases} \tag{47}$$

where $\cos\theta' = (1/n_2)\sqrt{n_2^2-n_1^2\sin^2\theta}$ and $\sin\theta' = (n_1/n_2)\sin\theta$.

Here we have used the following identities:

$$1+r_s^{21}(\theta') = 1-r_s^{12}(\theta),\quad 1-r_s^{21}(\theta') = 1+r_s^{12}(\theta),$$
$$t_s^{21}(\theta') = 1-r_s^{12}(\theta),$$
$$1+r_p^{21}(\theta') = 1-r_p^{12}(\theta),\quad 1-r_p^{21}(\theta') = 1+r_p^{12}(\theta),$$
$$t_p^{21}(\theta') = \frac{n_2}{n_1}[1-r_p^{12}(\theta)].$$

G. Result for integrated scattering TIS

Total integrated scattering (TIS) is an important tool for quality analysis of optical surfaces. By measuring TIS we determine the total amount of light flux scattered by the probe in the reflection hemisphere. We obtain the TIS by spatially integrating the ARS in the half space containing the direction of reflection. During measurement integration is performed using a Coblentz sphere or an Ulbricht sphere as spatially integrating element. Descriptions of experimental setups are found in Refs. 16, 17, and 2.

Following Elson[18] we assume a surface the spatial scattering distribution of which is limited to small angle scattering. Assuming small incidence angles of the illuminating light, we obtain for the total scattering loss of the front surface

$$\left(\frac{P_s}{P_0}\right)^f = \int_{\theta=0}^{\pi/2}\int_{\phi=0}^{2\pi}\mathcal{S}^f(\theta,\phi)\sin\theta\,d\theta\,d\phi = R^{12}\left(\frac{4\pi}{\lambda}\delta_{\text{rms}}^f\right)^2,$$

with

$$\delta_{\text{rms}}^2 = \frac{1}{(2\pi)^2}\int_{k_y}\int_{k_x}G(k_x,k_y)dk_xdk_y$$

in k space, or

$$\delta_{\text{rms}}^2 = \frac{1}{A}\int_A\int|S(x',y')|^2dx'dy'$$

in surface coordinates. R^{12} is the reflected power coefficient of the air-material interface and δ_{rms} is the rms surface roughness of the interface.

With the same assumptions the total scattering loss of the back surface can be calculated:

$$\left(\frac{P_s}{P_0}\right)^b = \int_{\theta=0}^{\pi/2}\int_{\phi=0}^{2\pi}\mathcal{S}^b(\theta,\phi)\sin\theta\,d\theta\,d\phi = R^{12}(1-R^{12})^2n_2^2\left(\frac{4\pi}{\lambda}\delta_{\text{rms}}^b\right)^2. \tag{48}$$

The substrate material is assumed to be nonabsorbing. Since the TIS is defined as the total scattering loss divided by the reflected power coefficient of the surface, we obtain for the total scattering loss of the substrate

$$\frac{P_s}{P_0} = R^{12}\mathcal{T}^f + R^{12}(1-R^{12})^2 n_2^2 \mathcal{T}^b. \tag{49}$$

To obtain correct experimental data in TIS measurements, the scattered light of both surfaces has to strike the detector. Since a Coblentz sphere is an imaging system, there is the problem of collecting the scattered light of both surfaces on the detector. Especially for thick substrates additional analysis has to be done to determine the amount of scattered light that is not detected and caused by the surface that is out of focus. For this reason an Ulbricht-sphere-type of TIS instrument is better suited to measure the total scatter loss of a transparent substrate.

Using the measuring technique described above we can determine the TIS and the corresponding rms surface roughness for the interfaces I and II separately:

$$\begin{pmatrix} \mathcal{T}_{\mathrm{I}} \\ \mathcal{T}_{\mathrm{II}} \end{pmatrix} = \left[R^{12} - R^{12}(1-R^{12})^4 n_2^4\right]^{-1} \begin{pmatrix} 1 & -(1-R^{12})n_2^2 \\ -(1-R^{12})n_2^2 & 1 \end{pmatrix} \begin{pmatrix} \left(\frac{P_s}{P_0}\right)_{\mathrm{I}} \\ \left(\frac{P_s}{P_0}\right)_{\mathrm{II}} \end{pmatrix},$$

$$\mathcal{T} = \frac{P_s}{RP_0 + P_s} \approx \frac{P_s}{RP_0}, \qquad \mathcal{T}_{\mathrm{I,II}} = \left(\frac{4\pi}{\lambda}\delta_{\mathrm{rms}}^{\mathrm{I,II}}\right)^2. \tag{50}$$

Or, assuming equally polished surfaces with mean rms roughness $\hat{\delta}_{\mathrm{rms}}$ we obtain

$$\hat{\mathcal{T}} = \left\{R^{12}\left(1 + [1-R^{12}]^2 n_2^2\right)\right\}^{-1} \frac{P_s}{P_0}. \tag{51}$$

Thus we can easily calculate the surface roughness of the substrate interfaces from integrated scatter measurements.

III. SUMMARY

In this paper a model is described that determines the measurable scattering distribution of a transparent glass substrate consisting of two slightly rough interfaces. Starting from the replacement of the actual surface by a flat interface and a surface current distribution in this plane, we calculate the scattered far fields caused by the rough interface. The scattered fields are calculated directly using the vector potential caused by the surface current distribution. By considering the reaction of the flat interface on the scattered field, a result for the ARS of an opaque surface is obtained that is identical to the the result found by other authors. Knowing the fundamentals of the scattering process, we are able to apply the theoretical model to the scattering process at the back surface of the substrate. The result is that the back surface contributes a greater amount of scattered light than the front surface when the surfaces are assumed to have equal surface roughness. This result has been confirmed by measurement. The difference in the scattering contributions can be explained by the different phase shifts that occur when the scattered field is reflected off the two interfaces. With the result of the theory, power-spectral-density functions of the substrate surfaces can be calculated from ARS measurement, and rms roughness can be calculated from TIS measurement using an Ulbricht sphere. Thus surface roughness analysis can be performed from scatter measurements of uncoated transparent substrates. The calculation method is restricted to substrates with low bulk scattering with respect to surface scattering, since bulk scattering is not considered in this theory.

ACKNOWLEDGMENTS

This work was financially supported by the Deutsche Forschungsgemeinschaft (DFG).

APPENDIX A

Fresnel amplitude coefficients of reflection and transmission for an interface separating two nonmagnetic media with refractive indices n_1 and n_2 are

$$r_s^{12}(\theta_1) = \frac{n_1\cos\theta_1 - \sqrt{n_2^2 - n_1^2\sin^2\theta_1}}{n_1\cos\theta_1 + \sqrt{n_2^2 - n_1^2\sin^2\theta_1}}, \tag{A1}$$

$$r_p^{12}(\theta_1) = \frac{n_2^2\cos\theta_1 - n_1\sqrt{n_2^2 - n_1^2\sin^2\theta_1}}{n_2^2\cos\theta_1 + n_1\sqrt{n_2^2 - n_1^2\sin^2\theta_1}}, \tag{A2}$$

$$t_s^{12}(\theta_1) = \frac{2n_1\cos\theta_1}{n_1\cos\theta_1 + \sqrt{n_2^2 - n_1^2\sin^2\theta_1}}, \tag{A3}$$

$$t_p^{12}(\theta_1) = \frac{2n_1 n_2\cos\theta_1}{n_2^2\cos\theta_1 + n_1\sqrt{n_2^2 - n_1^2\sin^2\theta_1}}. \tag{A4}$$

APPENDIX B

In the described model the scattered fields are calculated in the different media, and the transitions of the fields through the interfaces are considered. We have to determine the scattering direction in the respective medium caused by a Fourier component (wave vector $\vec{k}_l$)

of the surface. With a scattering direction $\vec{k}$ (related scattering angles θ, ϕ) given in medium 1, the corresponding wave vector $\vec{k}_l$ in the sample surface is as follows:

$$\vec{k}_l = \vec{k}_\perp - \vec{k}_\perp^{(0)} = \frac{\omega}{c} n_1 (\sin\theta\, \vec{e}_\Phi - \sin\theta_0\, \vec{e}_{\Phi_0}). \qquad \text{(B1)}$$

In medium 2 the respective Fourier component gives rise to a scattering direction $\vec{k}'$ (scattering angles θ', ϕ) since the wave number has changed:

$$\vec{k}_l = \vec{k}'_\perp - \vec{k}_\perp^{(0)'} = \frac{\omega}{c} n_2 (\sin\theta'\, \vec{e}_\Phi - \sin\theta'_0\, \vec{e}_{\Phi_0}). \qquad \text{(B2)}$$

As the scattered light is detected in medium 1, we obtain according to Snell's law for refraction $n_1 \sin\theta_0 = n_2 \sin\theta'_0$ and $n_1 \sin\theta = n_2 \sin\theta'$. Hence $\vec{k}_\perp^{(0)} - \vec{k}_\perp = \vec{k}_\perp^{(0)'} - \vec{k}'_\perp$. Thus we need not change the argument of the surface PSD's. However, when calculating the coefficients of reflection and transmission the different scattering angles θ in medium 1 and θ' in medium 2 have to be considered.

[1] C. Amra, C. Grezes-Besset, P. Roche, and Emile Pelletier, Appl. Opt. **28**, 2723 (1989).

[2] O. Kienzle, J. C. Staub, and T. Tschudi, Meas. Sci. Technol. (to be published).

[3] L. D. Mattsson, in *Workshop on Optical Fabrication and Testing Technical Digest* (Optical Society of America, Washington, D.C., 1987), Vol. 19, p. 85.

[4] E. Kroeger and E. Kretschmann, Z. Phys. **237**, 1 (1970).

[5] J. M. Elson, Opt. Eng. **18**, 2282 (1977).

[6] J. M. Elson, Appl. Opt. **16**, 2872 (1977).

[7] P. Bousquet, F. Flory, and P. Roche, J. Opt. Soc. Am. **71**, 115 (1981).

[8] In general, cross-correlation terms occur for scattering of systems consisting of more than one interface (Ref. 7). They describe interference effects of the scattered fields emerging from the different interfaces. For vanishing cross-correlation terms the scattering distribution is the sum of the scattering distributions of each interface weighted by the corresponding optical factor. Since the two sides of the substrate are polished individually, the cross-correlation term vanishes and the scattering distribution is the sum of the distributions of the two interfaces.

[9] A. A. Maradudin and D. L. Mills, Phys. Rev. B **11**, 1392 (1975).

[10] J. M. Elson, Phys. Rev. B **30**, 5460 (1984).

[11] J. D. Jackson, *Klassische Elektrodynamik*, 2nd ed. (de Gruyter, Berlin, 1982).

[12] H. J. Juranek, Z. Phys. **233**, 324 (1970).

[13] J. M. Elson, Phys. Rev. B **12**, 2541 (1975).

[14] E. L. Church, H. A. Jenkinson, and J. M. Zavada, Opt. Eng. **18**, 125 (1979).

[15] Oliver Kienzle, Diploma thesis, Technische Hochschule Darmstadt, 1993.

[16] John A. Detrio and Susan M. Miner, Opt. Eng. **24**, 479 (1985).

[17] Karl H. Guenther, Peter G. Wierer, and Jean M. Bennett, Appl. Opt. **23**, 3820 (1984).

[18] J. M. Elson, J. P. Rahn, and J. M. Bennett, Appl. Opt. **22**, 3207 (1983).

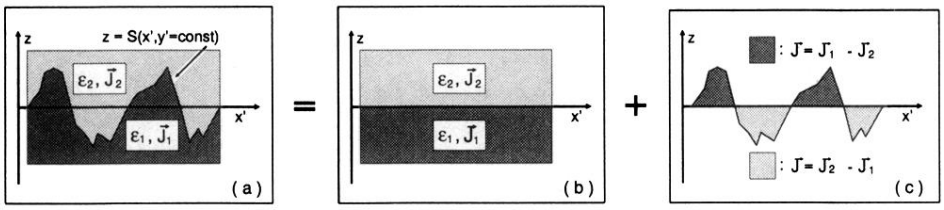

FIG. 1. Synthesis of the polarization current density distribution (CDD) at the actual interface (a) as superposition of the polarization CDD from an ideal flat interface (b) and the CDD (c). CDD (c) causes the scattered field.

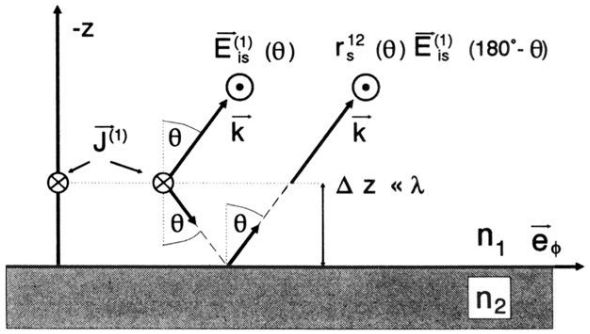

FIG. 4. Reaction of the flat interface $z = 0$ on the s-polarized scattered field $\vec{E}_{is}^{(1)}$. The surface CDD $\vec{J}^{(1)}$ is assumed to be located in medium 1, in distance $\Delta z \ll \lambda$ above the interface. The scattered field propagating in the direction $\vec{k}$ is the sum of the field emitted from $\vec{J}^{(1)}$ directly in direction θ, ϕ and the field emitted in direction $(180° - \theta)$, ϕ and reflected off the interface.